Lawrence Berkeley National Laboratory
Recent Work

Title
ELASTIC PROPERTIES OF MULTIPHASE CERAMIC SYSTEMS

Permalink
https://escholarship.org/uc/item/3n01j3rh
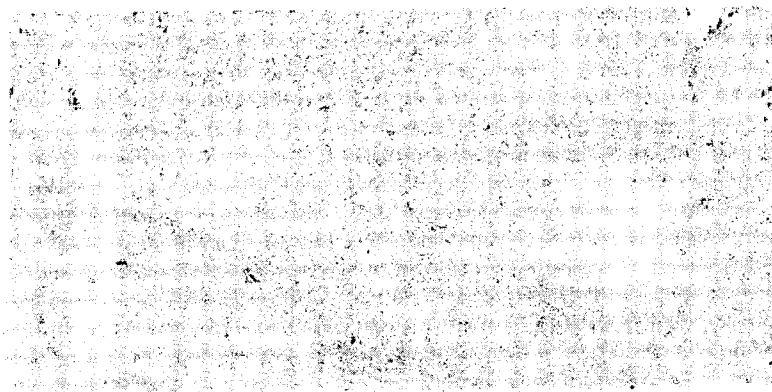
Authors
Hasselman, D.P.H.
Fulrath, R.M.

Publication Date
1965-09-22

University of California

Ernest O. Lawrence Radiation Laboratory

ELASTIC PROPERTIES OF MULTIPHASE CERAMIC SYSTEMS

Berkeley, California

DISCLAIMER

UCRL-16360

UNIVERSITY OF CALIFORNIA

Lawrence Radiation Laboratory
Berkeley, California

AEC Contract No. W-7405-eng-48

ELASTIC PROPERTIES OF MULTIPHASE CERAMIC SYSTEMS

D. P. H. Hasselman and R. M. Fulrath

September 22, 1965

ELASTIC PROPERTIES OF MULTIPHASE CERAMIC SYSTEMS

D. P. H. Hasselman and R. M. Fulrath

Inorganic Materials Research Division, Lawrence Radiation Laboratory,
and Department of Mineral Technology, College of Engineering,
University of California, Berkeley, California

September 22, 1965

ABSTRACT

The development of many multicomponent ceramic materials has focused attention on the macroscopic elastic behavior of such composite materials.

The present paper discusses the effect of various types of dispersions on Young's modulus of an isotropic homogeneous matrix in terms of the elastic properties, volume fractions, and particle shape of the dispersant. A short review is given of the theoretical contributions in the literature. The multicomponent materials investigated consisted of a sodium borosilicate glass containing (a) small volume fractions of spherical pores, (b) crushed sapphire, and (c) spherical particles of tungsten. Young's modulus of elasticity was determined by a flexural resonance technique. Experimental results of this investigation and other comparable work are compared with theory.

I.   INTRODUCTION

The recent development of many multicomponent materials of major technological importance, such as glass fiber-reinforced plastics, cermets, glass-ceramics, and many others, has focused attention on the elastic behavior of such composite systems. A special case of the elastic properties of composites is the effect of porosity on the elastic properties of many refractory materials. Special manufacturing techniques used for these materials (i.e., sintering, hot-pressing) usually do not result in complete densification.

Considerable theoretical work has appeared in the literature to predict the elastic properties of multicomponent systems in terms of the elastic properties, the volume fraction, and distribution of the components of the composite. Paul[1] derived upper and lower bounds between which the elastic moduli must fall regardless of the phase distribution. Mackenzie[2] calculated the effect of small fractions of spherical holes on the elastic moduli of a homogeneous matrix. Dewey[3] and Krivoglaz and Cherevko[4] derived expressions for the elastic moduli of matrices containing small amounts of spherical inclusions with arbitrary elastic properties. The solutions of Krivoglaz and Cherevko[4] were extended to apply to composites with arbitrary volume fractions of the components but small differences in elastic properties. Kerner[5] and Hashin[6] gave approximate solutions for the elastic properties containing arbitrary volume fractions of spherical particles with arbitrary elastic properties. For this system Hashin[6] also gave upper and lower bounds on the overall elastic moduli. Paul[1] presented a "strength-of-

materials" solution for a matrix containing cubical dispersions. Hashin and Shtrikman[7] calculated upper and lower bounds for the elastic moduli for a matrix containing dispersions of arbitrary phase geometry. Finally, the solutions of Hofferberth[8] and of Hashin and Rosen[9] for the moduli of matrices containing various arrays of fibers should also be mentioned. In all the theoretical derivations, perfect bonding between phases was always assumed.

Experimental data for the elastic moduli of multicomponent systems appear to be limited. Numerous data have appeared in the literature for the system tungsten carbide-cobalt.[10-14] Gurland[15] investigated the effect of various types of dispersion on the elastic moduli of silver. Tinklepaugh and Crandall[16] list elastic property values for many types of cermets. Mel'nichuk et al.[17] determined elastic moduli for the system chromium carbide-nickel. The system zirconium carbide containing a dispersed phase of graphite was investigated by Hasselman.[18] Because of the technological importance, considerable experimental[19-25] and empirical work[26-31] has been done to determine and predict the effect of porosity on the elastic moduli of many ceramic materials. In general, a large discrepancy was observed between the experimental effect of porosity on elastic moduli and the theoretically predicted effect using as a mechanical model a matrix containing spherical pores. This discrepancy was attributed by Spinner et al.[23] to the fact that the actual pore shape deviates from the idealized spherical pore shape assumed for the theoretical calculations. In general, the phase geometry (microstructure) of the multicomponent materials investigated does

not lend itself well to description and generally deviates sharply from the mechanical models on which the theoretical equations are based. As a consequence, the interpretation of the experimental data and the verification of the theoretical expressions become rather difficult, as well as questionable.

It is the purpose of this paper to present and compare with theory experimental data for the elastic properties of multicomponent systems consisting of a continuous matrix containing dispersions with controlled dispersion particle size, shape, and volume fraction. The systems selected consisted of a glass matrix containing (a) spherical pores, (b) crushed saphhire, and (c) spherical particles of tungsten. The use of a glass as the matrix materials gives the assurance of a continuous phase which is homogeneous and pore-free. The types of dispersants were selected to give as large a difference as possible between the elastic properties of the matrix and dispersant. Large variations in experimental data of the composite elastic properties are thereby attained and should facilitate the interpretation and comparison of experimental data and theoretical predictions.

II. EXPERIMENTAL

A. Materials

The matrix selected consisted of a sodium borosilicate glass of composition 16% Na_2O, 14% B_2O_3, and 70% SiO_2 by weight. The dispersants consisted of a tungsten powder spheroidized in a plasma jet with particle size approximately 30μ and crushed sapphire of particle size approximately 50μ. The third dispersant consisted of spherical pores.

B. Specimen Preparation

The glass specimens containing spherical holes were prepared by melting in a platinum crucible at 1300°C an intimate mixture of sodium carbonate, boric acid, and silica. The formation of carbon dioxide and water provided the gases for bubble formation. The relative amount of bubbles in the melt was an inverse function of the length of time the crucible was held at temperature. The melt was held at temperature from about 20 to 40 min, depending on the bubble content desired. Specimens (5 by 1/2 by 1/2 in.) were cast in suitable graphite molds preheated to 650°C. During casting, the bubbles retained their spherical shape under the influence of surface tension. The molds were allowed to cool to room temperature after which the specimens were removed. Pore content ranged from about 0.5 to 2.5 vol %. Figure 1 shows a photomicrograph of a specimen containing 1.62 vol % porosity. The porosity of each specimen was calculated from the true glass density and the bulk density calculated from the mass and dimensions of each specimen. The true glass density was determined by measuring the density of crushed glass by a pycnometer technique. The cast specimens were cut into specimens approximately 4 in. long, 1/2 in. wide, and 1/4 in. thick by means of a high-precision diamond saw.

Glass-sapphire and glass-tungsten specimens were prepared by vacuum hot-pressing at 725°C for 10 min, intimate mixtures of the components in powder form into 2 in. diam by 1/4 in. thick disks using suitable graphite dies. The particle size of the glass powder, prepared by crushing and milling, was approximately 3 to 5μ. Figure 2 shows the

microstructure of a glass alumina composite containing 30 vol % alumina.

Similarly, Fig. 3 shows the structure of a glass-tungsten compact containing 40 vol % tungsten. Two specimens approximately 1-3/4 by 1/4 by 1/4 in. were cut from each disk. Dimensional precision was approximately 0.001 in., requiring no further surface treatment.

C. Elasticity Measurements

Elastic moduli were measured at room temperature using the resonance technique described by Spinner and Tefft,[32] based on the original paper by Pickett.[33] The validity of this method was investigated in great detail by a number of investigators[34-36] and for the specimen size and shape should give an experimental error no greater than 0.4%.[21] By determining the resonant frequency in the "flatwise and edgewise" vibration, two values of Young's modulus were obtained per specimen. Calculations were made with tables compiled for this purpose.[37] The shear modulus was calculated by the more precise expression for the shape factor involved given by Spinner and Tefft.[32] The shear modulus of the glass-sapphire and glass-tungsten systems could not be determined due to the frequency limitation of the instrument employed.

III. EXPERIMENTAL RESULTS, DISCUSSION, AND CONCLUSIONS

Figure 4 shows the experimental results of Young's modulus and the shear modulus of the glass specimens containing spherical pores. Included in Fig. 4 are the values of the index of refraction. Since within the accuracy of measurement (±0.0002) the index of refraction was independent of pore content, it appeared to be reasonable that the

changes in Young's modulus and shear modulus could be attributed

primarily to the presence of the pores.

In order to compare experimental results with theory, the data

shown in Fig. 4 by the method of least squares were fitted to the

linear expression of the form

$$E = E_o (1 - \alpha_E P) \tag{1}$$

and

$$G = G_o (1 - \alpha_G P) , \tag{2}$$

where E and G are the Young's modulus and shear modulus, respectively,

of the porous specimens, E_o and G_o represent the moduli of the nonporous

material, α is a constant, and P is the volume fraction porosity.

The theoretical value of α_E was calculated from the solutions for

the effect of spherical porosity on shear modulus and bulk modulus.[2-4,6]

This resulted in

$$\alpha_E = \frac{3(9 + 5 \nu_o)(1 - \nu_o)}{2(7 - 5 \nu_o)} , \tag{3}$$

where ν_o is Poisson's ratio of the nonporous material.

The theoretical value of α_G equals

$$\alpha_G = \frac{15(1 - \nu_o)}{(7 - 5 \nu_o)} .$$

Substitution of the value of Poisson's ratio of the glass ($\nu_o \approx$

0.20) results in theoretical values of $\alpha_E = \alpha_G = 2.00$. The experimental

values for α_E and α_G determined by the curve-fitting technique for α_E

and α_G were found to be 2.06 and 1.99 with probable errors of 0.06 and

0.09, respectively. It appears, therefore, that good agreement exists between theory and experiment at least for the type of material and range of porosity investigated. It appears highly probable, therefore, that the observed discrepancy between theory and experiment for the effect of porosity in sintered and hot-pressed ceramics can be attributed to the fact that the actual pore shape deviates from the idealized pore shape assumed in the theoretical derivations, in agreement with the conclusion of Spinner et al.[23]

A new estimate can be made of the effect of porosity in elastic properties on the basis of Hashin and Rosen's[9] calculation of the elastic properties of matrices containing arrays of parallel cylindrical fibers. In Hashin and Rosen's solution, setting the elastic properties of the fibers identically equal to zero results in a matrix containing parallel cylindrical pores. As expected, considerable elastic anisotropy is obtained. Young's modulus parallel to the pores follows the law of mixtures. Hashin and Rosen's results perpendicular to the pores are expressed in terms of a bulk modulus and upper and lower bounds for the shear modulus, from which upper and lower bounds for Young's modulus can be computed directly. Figure 5 illustrates the results for a matrix with Poisson's ratio = 0.25. For comparison, included in the figure are the upper and lower bounds for a matrix ($\nu_o = 0.25$) containing spherical pores.[6] Also included are the experimental data for alumina as computed by Knudsen[27] expressed in terms of the experimental equation of Spriggs[26] given by $E = E_o e^{-3.95P}$, where E and E_o are Young's modulus of the nonporous body, respectively, and P is the porosity. The results

in Fig. 5 indicate that the predicted curves for cylindrical porosity fall well below these for spherical porosity. But for a narrow region at low porosity, the experimental curve falls between the upper and lower bound for cylindrical porosity. For porosities less than about 15% the discrepancy between the experimental curve and the lower bound for the cylindrical porosity amounts to no more than a few percent. In experimental bodies, manufactured by sintering or hot-pressing, at least part of the porosity can be considered to be cylindrical, especially at higher porosities where the pores tend to be interconnected (open porosity) rather than isolated (closed porosity). In view of this and the results present in Fig. 5, it is suggested that a matrix containing parallel cylindrical pores oriented perpendicularly to the applied stress might represent a better mechanical model for the prediction of the effect of porosity on Young's modulus of sintered and hot-pressed ceramics than a matrix containing spherical pores.

Figure 6 shows the experimental results together with the theoretical curve for Young's modulus of the glass containing crushed sapphire as the dispersed phase. Table I lists the actual experimental data. To facilitate comparison between theory and experiment, Table I also lists the calculated data for the theoretical curves. Young's modulus for the glass was found to be 805 kilobars, which is slightly higher than the value which can be obtained by extrapolating to zero porosity data for Young's modulus for the glass specimens containing spherical pores as shown in Fig. 4. This discrepancy probably can be attributed to differences in thermal history. For the theoretical calculations

Poisson's ratio (ν_o) for the glass was taken as 0.197 obtained from the data presented in Fig. 4. Elastic property values for the alumina were: shear modulus = 1635 kilobars[29] and Poisson's ratio (ν_o) = 0.257.[29] Young's modulus for the predictions of Hashin and Shtrikman[7] and of Hashin[6] was calculated from the corresponding equations for the bulk and shear modulus. Kerner's[5] expression is identical to Hashin and Shtrikman's[7] lower bound for arbitrary phase geometry and Hashin's[6] approximate solution for spherical phase geometry, and therefore was not included. The apparent decrease in Young's modulus at approximately 50 vol % alumina is probably due to a lack of complete densification because of alumina particle-to-particle contact. It is of interest to note that the experimental results fall well below the law of mixtures (Paul's[1] upper bound). For this particular system, the experimental results appear to agree very well with Hashin and Shtrikman's[7] lower bound for arbitrary phase geometry.

Figure 7 shows the experimental and theoretical results for Young's modulus of the glass matrix containing spherical tungsten particles as the dispersant. Table II lists the numerical values of the calculated and experimental data. For the theoretical calculations, tungsten elastic properties were taken as Young's modulus = 3550 kilobars and shear modulus = 1481 kilobars.[38] Experimental results fall between Hashin's upper bound for spherical phase geometry and Hashin and Shtrikman's lower bound for arbitrary phase geometry, as would be expected from theory. It is of interest to note here that the data for the glass-sapphire system lie in the same relative position as the data

for the glass-tungsten system. It appears, therefore, that for this type of two-phase system, composed of a matrix containing random dispersions with Young's modulus higher than the matrix, dispersion shape, at least macroscopically, plays little or no role.

It is of interest to compare the results of the systems glass-sapphire and glass-tungsten with the results for the system zirconium carbide containing a dispersed phase of graphite.[18] This system is characterized in that the dispersed phase has a much lower Young's modulus than the zirconium carbide matrix, whereas the reverse is true for the glass-sapphire and glass-tungsten system. Figure 8 shows the experimental results together with the calculated curves. It is immediately evident that enormous differences exist between the various predicted curves. The experimental data appear to be given best by Hashin's[6] lower bound for spherical phase geometry. Hashin and Shtrikman's[7] lower bound for arbitrary phase geometry, which rather accurately predicts the elastic moduli for the glass-sapphire and glass-tungsten systems, for the system zirconium carbide graphite predicts values only about one-quarter of these observed. It is clear that additional experimental and theoretical work is required for this and analogous systems.

It is also of interest to observe that the "strength-of-materials" expression derived by Paul[1] for a matrix containing cubical inclusions for all systems shown in Figs. 6, 7, and 8 consistently predicts values which are higher than these observed. Paul's[1] equation also predicts elastic moduli higher than observed when applied to a matrix containing porosity at the dispersed phase, as is easily verified. On the other

hand, Paul's expression has been quite successfully applied to the
system tungsten carbide-cobalt and to multicomponent systems composed
of silver containing various materials as the dispersant. It should be
noted here that as the relative differences in elastic moduli of the
components decrease, the various theoretical curves will fall closer
together and will virtually coincide for systems with little or no
differences in elastic properties of the components. From the experi-
mental data and the various theoretical curves presented, it appears
that in determining the elastic moduli of continuous matrix-dispersed
phase two-phase systems that the component with the lower elastic modulus
is the governing factor. When a lower Young's modulus dispersant is
added to a higher Young's modulus matrix, a rapid decrease with volume
content dispersed phase is generally observed. Conversely, however, if
a high Young's modulus dispersed phase is added to a matrix with lower
Young's modulus, Young's modulus only rises gradually with increasing
dispersed phase content. The authors conclude that for the type of
system investigated in the present paper elastic properties can be pre-
dicted to a reasonable degree of reliability. It should be pointed out,
however, that predictions of the elastic properties of multicomponent
ceramic systems is handicapped due to the fact that very few reliable
data exist for the elastic properties of most ceramic materials, alumina
and magnesia perhaps being the only exception. Data reported in the
literature are often obtained using porous samples of unknown micro-
structure, purity, and thermal history and manufacturing technique.
Considerable experimental work is still required to more firmly establish
elastic property data for most ceramics.

ACKNOWLEDGMENTS

The authors are indebted to George Dahl for the photomicrographs and John Frease for experimental assistance.

REFERENCES

1. B. Paul, "Prediction of Elastic Constants of Multi-phase Materials," Trans. AIME, 218 [1] 36-41 (1960).

2. J. K. Mackenzie, "The Elastic Constants of a Solid Containing Spherical Holes," Proc. Phys. Soc. (London), B63, 2-11 (1950).

3. J. M. Dewey, "The Elastic Constants of Materials Loaded with Non-Rigid Fillers," J. Appl. Phys., 18, 578 (1948).

4. M. A. Krivoglaz and A. S. Cherevko, "On the Elastic Moduli of a Two-Phase Solid," Phys. Metals and Metallography, 8 [2] 161-164 (1959).

5. E. H. Kerner, "Elastic and Thermoelastic Properties of Composite Media," Proc. Phys. Soc. (London), B69, 808-813 (1956).

6. Z. Hashin, "Elastic Moduli of Heterogeneous Materials," J. Appl. Mech., 29 [1] 143-150 (1962).

7. Z. Hashin and S. Shtrikman, "A Variational Approach to the Theory of the Elastic Behavior of Multiphase Materials," J. Mech. Phys. Solids, [2] 127-140 (1963).

8. W. Hofferberth, "Zum Elastizitätzgesetz für den Verbund-körper Gummi-Textil," Gummi und Asbest, 9, 240, 242, 244-247 (1956).

9. Z. Hashin and B. W. Rosen, "The Elastic Moduli of Fiber-Reinforced Materials," J. Appl. Mech., 2, 223-232 (1965).

10. W. Köster and W. Rauscher, "Beziehungen zwischen dem Elastizitätzmodul von Zweistoff Legierungen und ihrem Aufbau, Zeit. Metallk., 39, 111-122 (1948).

11. E. Lardner and N. B. McGregor, "Determination of Elastic Constants and Stress/Strain Relationship to Fracture of Sintered Tungsten Carbide-Cobalt Alloys," J. Inst. Metals, 80, 369-374 (1951-52).

12. E. Ammann and J. Hinüber, Stahl u. Eisen, 71, 1081 (1951).

13. C. Nishimatsu and J. Gurland, "Experimental Survey of the Deformation of a Brittle-ductile Two-phase Alloy System; WC-Co," Technical Report No. 2, Division of Engineering, Brown University, Sept. 1958.

14. P. Schwarzkopf and R. Kieffer, Cemented Carbides. The Macmillan Company, New York, 1960.

15. J. Gurland, "Comparison of Dispersion Hardening in Four Silver-Base Alloys of Equivalent Composition," Trans. AIME, 221 [4] 407-408 (1961).

16. J. R. Tinklepaugh and W. B. Crandall, Cermets. Reinhold Publishing Corporation, New York, 1960. 239 pp.

17. P. I. Mel'nichuk, V. N. Klimenko, and A. B. Lyrshchenko, "Determination of the Modulus of Elasticity in Alloys of Chromium Carbide-Nickel," Phys. Metals and Metallography, 9, 106 (1960).

18. D. P. H. Hasselman, "Experimental and Calculated Young's Moduli of Zirconium Carbide Containing a Dispersed Phase of Graphite," J. Am. Ceram. Soc., 46 [2] 103-104 (1963).

19. H. Z. Schofield, J. F. Lynch, and W. H. Duckworth, "Fundamental Studies of Ceramic Materials," Final Summary Report, Battelle Memorial Institute to Office of Naval Research, Navy Dept. Contract No. N5 ORL-111, March 31, 1949.

20. R. L. Coble and W. D. Kingery, "Effect of Porosity on Physical Properties of Sintered Alumina," J. Am. Ceram. Soc., 39 [11] 377-385 (1956).

21. S. M. Lang, "Properties of High-Temperature Ceramics and Cermets--Elasticity and Density at Room Temperature," Natl. Bur. Std. Monograph No. 6, 1960.

22. W. B. Crandall, D. H. Chung, and T. J. Grey, "The Mechanical Properties of Ultra-Fine Hot-Pressed Alumina," pp. 349-379 in Mechanical Properties of Engineering Ceramics. Edited by W. W. Kriegel and H. Palmour, III. Interscience Publishers, New York-London, 1961.

23. S. Spinner, F. P. Knudsen, and L. Stone, "Elastic Constant-Porosity Relations for Polycrystalline Thoria," J. Res. Natl. Bur. Std., 67 [1] 39-46 (1963).

24. R. E. Gannon, G. M. Harris, and T. Vasilos, "Effect of Porosity on Mechanical, Thermal and Dielectric Properties of Fused Silica," Am. Ceram. Soc. Bull., 44 [5] 460 (1965).

25. R. E. Fryxell and B. A. Chandler, "Creep, Strength, Expansion and Elastic Moduli of Sintered BeO as a Function of Grain Size, Porosity and Grain Orientation," J. Am. Ceram. Soc., 47 [6] 283-291 (1964).

26. R. M. Spriggs, "Expression for Effect of Porosity on Elastic Modulus of Polycrystalline Refractory Materials, Particularly Aluminum Oxide," J. Am. Ceram. Soc., 44 [12] 628-629 (1961).

27. F. P. Knudsen, "Effect of Porosity on Young's Modulus of Alumina," J. Am. Ceram. Soc., 45 [2] 94-95 (1962).

28. D. P. H. Hasselman, "On the Porosity Dependence of the Elastic Moduli of Polycrystalline Refractory Materials," J. Am. Ceram. Soc., 45 [9] 452-453 (1962).

29. R. M. Spriggs and L. A. Brisette, "Expression for Shear Modulus and Poisson's Ratio of Refractory Oxides," J. Am. Ceram. Soc., 45 [4] 198-199 (1962).

30. R. M. Spriggs, "Effect of Open and Closed Pores on Elastic Moduli of Polycrystalline Alumina," J. Am. Ceram. Soc., 45 [9] 454 (1962).

31. R. S. Piatasik and D. P. H. Hasselman, "Effect of Open and Closed Pores on Young's Modulus of Polycrystalline Ceramics," J. Am. Ceram. Soc., 47 [1] 50-51 (1964).

32. S. Spinner and W. E. Tefft, "Method for Determining Mechanical Resonance Frequencies and for Calculating Elastic Moduli from These Frequencies," Am. Soc. Testing Mater. Proc., 61, 1221-1238 (1961).

33. G. Pickett, "Equations for Computing Elastic Constants from Flexural and Torsional Resonant Frequencies of Vibrations of Prisms and Cylinders," Am. Soc. Testing Mater. Proc., 45, 846 (1945).

34. S. Spinner and R. C. Valore, Jr., "Comparison of Theoretical and Empirical Relations Between the Shear Modulus and Torsional Resonance Frequencies for Bars of Rectangular Cross Section," J. Res. Natl. Bur. Std., 60 [5] 459-464 (1958).

35. S. Spinner, T. W. Reichard, and W. E. Tefft, "A Comparison of Experimental and Theoretical Relations Between Young's Modulus and the Flexural and Longitudinal Resonance Frequencies of Uniform Bars," J. Res. Natl. Bur. Std., 64A [2] 147 (1960).

36. W. E. Tefft and S. Spinner, "Torsional Resonance Vibrations of Uniform Bars of Square Cross Section," J. Res. Natl. Bur. Std., 65A [3] 167-171 (1961).

37. D. P. H. Hasselman, "Tables for Computation of Shear Modulus and Young's Modulus of Elasticity from Resonant Frequencies of Rectangular Prisms," The Carborundum Company, Niagara Falls, New York, 1962. 195 pp.

38. <u>Handbook of Chemistry and Physics</u>, 36th edition, p. 1976. Chemical

Rubber Publishing Co., 1954-55.

Table I. Calculated and experimental effect of alumina dispersions
on Young's modulus of a sodium borosilicate glass (E_o = 805 kilobars)

Volume percent Al_2O_3	Spherical phase geometry[*]			Arbitrary phase geometry[†]		Paul[‡]			Experimental
	Upper bound	Lower bound	Approximate	Upper bound	Lower bound	Upper bound	Lower bound	Cubical inclusion	
10	925	912	920	1011	920	1137	870	1031	924 ± 4[**]
20	1069	1027	1057	1235	1057	1470	960	1225	1071 ± 5
30	1238	1163	1209	1479	1209	1802	1053	1428	1228 ± 5
40	1434	1330	1397	1748	1397	2135	1185	1641	1447 ± 14
45	--	--	--	--	--	--	--	--	1585 ± 10
50	1665	1542	1620	2043	1620	2467	1345	1891	1678 ± 13
55	--	--	--	--	--	--	--	--	1372[††] ± 13

* Reference 2.

† Reference 3.

‡ Reference 1.

** Standard deviation.

†† Approximately 9.6% porosity.

Table II. Calculated and observed effect of spherical tungsten dispersion on Young's modulus of a sodium borosilicate glass (E_0 = 805 kilobars)

Volume percent tungsten	Spherical phase geometry*			Arbitrary phase geometry†		Paul‡			Observed
	Upper bound	Lower bound	Approximate**	Upper bound	Lower bound**	Upper bound	Lower bound	Cubical inclusion	
10	918	907	914	982	914	1080	870	1001	909 ± 14††
20	1053	1015	1039	1172	1039	1354	953	1186	1055 ± 11
30	1206	1137	1182	1359	1182	1629	1049	1388	1180 ± 2
40	1386	1289	1349	1598	1349	1903	1166	1545	1375 ± 3
50	1592	1479	1548	1850	1548	2188	1312	1760	1599 ± 5

* Reference 6. ** Identical to Reference 5.

† Reference 7. †† Standard deviation.

‡ Reference 1.

FIGURE CAPTIONS

Fig. 1. Photomicrograph of sodium borosilicate glass specimen containing 1.62% porosity (X9).

Fig. 2. Microstructure of sodium borosilicate glass containing 30 vol % crushed sapphire (X100).

Fig. 3. Microstructure of sodium borosilicate glass containing 40 vol % spherical tungsten particles (X160).

Fig. 4. Young's modulus, shear modulus, and index of refraction of sodium borosilicate glass as a function of pore content.

Fig. 5. Calculated and observed effect of porosity on Young's modulus.

Fig. 6. Experimental and theoretical results for Young's modulus of sodium borosilicate glass as a function of the volume content of alumina particles.

Fig. 7. Experimental and theoretical results for Young's modulus of sodium borosilicate glass as a function of the volume content of spherical tungsten particles.

Fig. 8. Experimental and theoretical results for Young's modulus of zirconium carbide as a function of graphite content.
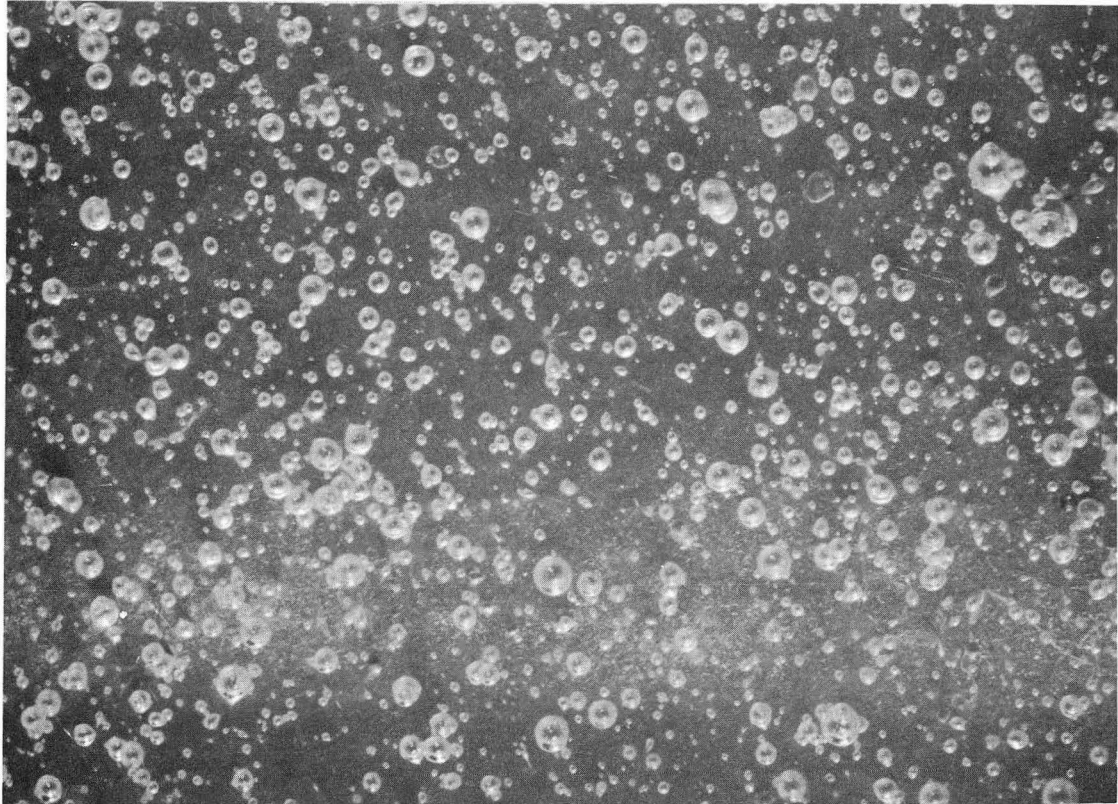
ZN-5258

Fig. 1

ZN-4559

Fig. 2

ZN-5001

Fig. 3

Fig. 4

MU-32031

MUB-6649

Fig. 5

—

Fig. 6

MUB-4610

Fig. 7

MUB-5833

MUB-5452

Fig. 8